Parameter Optimisation of a Viscothermal Time-Domain Model for Wind Instruments

Sebastian Schmutzhard,[1†] *Vasileios Chatziioannou,*[1] *Alex Hofmann*[1]

[1]Department of Music Acoustics (IWK), University of Music and Performing Arts, Vienna, Austria
[†]schmutzhard@mdw.ac.at

ABSTRACT

Viscothermal losses are vital for realistic numerical models of wind instruments. Numerical methods for modelling acoustic tubes that include viscothermal losses are well understood in the frequency domain for many years now. In this paper, motivated by the aim to numerically investigate note transitions on wind instruments, we study time-domain models for acoustic tubes. Time-domain modelling is better suited to such nonlinear, as well as time-varying systems. Recent methods use rational function approximation for including viscothermal losses in the time domain. We pursue the same approach and present a semi-analytic technique for the numerical integration of losses. Finally, in an attempt to accurately reproduce experimental findings, a time-domain bore optimisation routine is presented that includes the effect of viscothermal and radiation losses.

1. INTRODUCTION

Boundary layer losses need to be considered when modelling wave propagation in acoustic ducts. Physical modelling approaches including viscothermal losses are mostly performed in the frequency domain (see, e.g. [1, 2] or [3, Ch. 3.2.3]). The results of such frequency-domain approximations have been shown to be in good agreement with experimental measurements [4]. Nevertheless, it is sometimes required to model acoustic tubes in the time domain. This is particularly the case when systems with time-varying properties, as well as nonlinear systems need to be modelled [5].

In an attempt to simulate experimental arrangements for the investigation of transient processes in woodwind instruments (e.g. note transitions), it is therefore desirable to obtain accurate time-domain wave propagation models that include the effect of viscothermal losses. Recently, the use of rational function approximation has been presented to this end [6, 7, 5]. In this work, following the same approach, we present a semi-analytic technique for incorporating time-domain losses. The resulting wave propagation model can be coupled to a nonlinear excitation model that captures the interaction between the player's embouchure and the reed-mouthpiece system [8].

In order to accurately simulate experimental setups, a bore optimisation process is presented that, given either the input impedance or the impulse response of an acoustic tube, can arrive at an effective bore shape that represents the tube used in the experiment. Performing the optimisation in the time-domain ensures that the time-domain formulation of losses is consistent with subsequent attempts to model transient phenomena. Section 3 describes how both viscothermal losses as well as losses that occur at the open end of the tube due to sound radiation may be included in such models. Eventually optimisation may be performed in order to estimate model parameters (including bore geometry) based on time-domain pressure signals. Hence physics-based analysis attempts (see, e.g. [9]) may focus on characterising dynamic player-instrument interactions that occur at the mouthpiece during articulation.

2. MODELLING WAVE PROPAGATION IN TUBES

2.1. Frequency-domain model

We are considering a tube of length L and variable cross-sectional area $S = S(x), 0 \leq x \leq L$. The propagation of plane waves in tubular ducts, taking viscothermal losses into account, can be modelled in the frequency domain by [5, 10]

$$\partial_x P + ZV = 0, \tag{1a}$$

$$\partial_x (SV) + YSP = 0, \tag{1b}$$

where $P = P(\omega, x)$ is the acoustic pressure and $V = V(\omega, x)$ the particle velocity and ω denotes the frequency. The functions $Z = Z(\omega, x)$ and $Y = Y(\omega, x)$ are called the specific series impedance and the shunt addmitance, respectively. Specific formulas for Z and Y are given in [2].

To make the model complete, one has to impose boundary conditions at $x = 0$ and $x = L$. The left boundary, $x = 0$, is governed by a prescribed particle velocity $V(\omega, 0) = V_{\text{in}}(\omega)$ and the right, $x = L$, by a stipulated radiation impedance

$$Z_r(\omega) = \frac{P(\omega, L)}{S(L)V(\omega, L)}. \tag{2}$$

2.2. Time-domain model

In order to transfer the model (1) to the time domain, Z and Y can be split as [5]

$$Z = i\omega\rho + Z_v, \quad Y = \frac{i\omega}{\rho c^2} + Y_\theta, \tag{3}$$

where i denotes the imaginary unit, ρ the density of air and c the speed of sound in air. Since the cross-sectional area S does not depend on the time t, (1) transfers into

$$\partial_x p + \rho \partial_t v + z_v * v = 0, \tag{4a}$$

$$\partial_x (Sv) + \frac{S}{\rho c^2} \partial_t p + S y_\theta * p = 0, \tag{4b}$$

where $*$ denotes convolution with respect to the time variable t, and lower case function names refer to the time-domain versions of the capitalised functions. The boundary conditions in the time domain are given by $v(t,0) = v_{\text{in}}(t)$ at $x = 0$ and (2) transfers for $x = L$ to

$$p(t, L) = S(L)z_r * v(t, L). \tag{5}$$

In addition to the boundary conditions, we assume that the pressure p and the velocity v vanish for $t < 0$.

3. NUMERICAL SOLUTION OF THE TIME-DOMAIN MODEL

3.1. Semi-analytic computation of the losses

In order to deal with the convolutions $z_v * v$ and $y_\theta * p$ we pursue a similar approach as in [7] and approximate the functions Z_v and Y_θ, given in (3), by rational functions Z_v^K and Y_θ^K,

$$Z_v^K = R_0 + \sum_{k=1}^{K} \frac{R_k i\omega}{L_k + i\omega},\ Y_\theta^K = \sum_{k=1}^{K} \frac{G_k i\omega}{C_k + i\omega}. \tag{6}$$

One can show that for $\omega = 0$, $Y_\theta(0, x) = 0$, so a constant term in the approximation of Y_θ is not needed. R_k, L_k, G_k and C_k can be found by minimizing the differences $Z_v - Z_v^K$ and $Y_\theta - Y_\theta^K$ on a fixed set of frequencies by Newton's method [7]. Behold that the coefficients depend on the tube radius and hence on the spatial variable x, but in order to simplify notation, the x-dependency is not denoted. Hence, we approximate

$$z_v * v \approx R_0 v + \sum_{k=1}^{K} w_k \text{ and } y_\theta * p \approx \sum_{k=1}^{K} q_k \tag{7}$$

where the frequency-domain versions of w_k and q_k are given by the relations

$$W_k = \frac{R_k i\omega}{L_k + i\omega} V \text{ and } Q_k = \frac{G_k i\omega}{C_k + i\omega} P. \tag{8}$$

For $\lambda > 0$ and $H(t)$ denoting the Heaviside function, the Fourier transform of $H(t)e^{-\lambda t}$ is $\frac{1}{\lambda + i\omega}$, therefore

$$w_k(t) = R_k \int_0^t e^{-L_k(t-\tau)} \partial_t v(\tau) d\tau, \tag{9a}$$

$$q_k(t) = G_k \int_0^t e^{-C_k(t-\tau)} \partial_t p(\tau) d\tau. \tag{9b}$$

3.2. Computation of the boundary conditions

The boundary condition at $x = 0$ is $v(t, 0) = v_0(t)$. At the radiating end, we are using an approximation of Z_r of the form [3, Eq. (3.29b)]

$$Z_r(\omega) = \frac{i\omega R_r}{L_r + i\omega}. \tag{10}$$

The coefficients R_r and L_r depend on the radius and moreover on the flange of the tube. For example, the boundary condition discussed in [11, Eq. (9.9)] is of this form with $R_r = \frac{\rho}{S(L)\alpha_1}$ and $L_r = \frac{\alpha_2}{\alpha_1}$. In our study, we are considering flanged tube ends, hence the approximation (10) is accurate. When dealing with experimental results, more refined versions [12] should be considered, which will be optimised based on measured signals. With this approximation, the boundary condition at $x = L$ is, because of (5), given by the differential equation

$$S(L)R_r \partial_t v(t, L) = L_r p(t, L) + \partial_t p(t, L), \tag{11}$$

which can be discretised by finite differences.

3.3. Finite Difference scheme

We substitute (7) into (4) in order to arrive at

$$\partial_x p + \rho \partial_t v + R_0 v + \sum_{k=1}^{K} w_k = 0, \tag{12a}$$

$$\partial_x (Sv) + \frac{S}{\rho c^2} \partial_t p + S \sum_{k=1}^{K} q_k = 0. \tag{12b}$$

We compute approximations p_m^n and v_m^n to the solutions p and v of (12), respectively, at discrete points (t_n, x_m) in time and space, where $t_n = n\Delta_t$, $n = 0, 1, 2 \ldots$ and $x_m = m\Delta_x$ for $m = 0, \ldots, M$ and $L = M\Delta_x$, for fixed Δ_t and Δ_x.

One iteratively computes p_m^{n+1} and v_m^{n+1} from results obtained at previous time steps. In order to derive a discrete version of (12), we need the following discretisations of (9),

$$w_{k,m}^{n+1} \approx\ e^{-L_{k,m}\Delta_t} w_{k,m}^n + R_{k,m}(v_m^{n+1} - v_m^n) e^{-L_{k,m}\frac{\Delta_t}{2}}, \tag{13}$$

and

$$q_{k,m}^{n+1} \approx\ e^{-C_{k,m}\Delta_t} q_{k,m}^n + G_{k,m}(p_m^{n+1} - p_m^n) e^{-C_{k,m}\frac{\Delta_t}{2}}. \tag{14}$$

The boundary condition on the left gives for v_0^{n+1}

$$v_0^{n+1} = v_{\text{in}}^{n+1}. \tag{15}$$

Equation (12a) is discretised by finite differences and, using (13), one can compute $v_m^{n+1}, m = 1, \ldots, M$ from

$$\frac{p_m^n - p_{m-1}^n}{\Delta_x} + \rho \frac{v_m^{n+1} - v_m^n}{\Delta_t} + R_{0,m} v_m^{n+1} + \sum_{k=1}^{K} \left[e^{-L_{k,m}\Delta_t} w_{k,m}^n + R_{k,m}(v_m^{n+1} - v_m^n) e^{-L_{k,m}\frac{\Delta_t}{2}} \right] = 0. \tag{16}$$

Discretising (12b), and using (14), one computes p_m^{n+1}, $m = 0, \ldots, M-1$ from

$$\frac{S_{m+1} v_{m+1}^{n+1} - S_m v_m^{n+1}}{\Delta_x} + \frac{S_m}{\rho c^2} \frac{p_m^{n+1} - p_m^n}{\Delta_t} + S_m \sum_{k=1}^{K} \left[e^{-C_{k,m}\Delta_t} q_{k,m}^n + G_{k,m}(p_m^{n+1} - p_m^n) e^{-C_{k,m}\frac{\Delta_t}{2}} \right] = 0. \tag{17}$$

Taking finite differences in (11) yields for $m = M$

$$S_M R_r \frac{v_M^{n+1} - v_M^n}{\Delta_t} = L_r p_M^{n+1} + \frac{p_M^{n+1} - p_M^n}{\Delta_t}, \qquad (18)$$

from which p_M^{n+1} can be computed. Finally for $k = 1, \ldots, K$ and $m = 1, \ldots, M$, $w_{k,m}^{n+1}$ and $q_{k,m}^{n+1}$ are updated by (13) and (14), respectively.

4. BORE RECONSTRUCTION

In this section we use the time-domain model and its numerical implementation to estimate shape parameters of a tubular duct using the input impedance,

$$Z_{\text{in}}(\omega) = \frac{P(\omega, 0)}{S(0)V(\omega, 0)}. \qquad (19)$$

Having solved the numerical scheme (15) - (18) for timesteps $t_n = n\Delta_t$, $n = 0, \ldots, N-1$, we compute an approximation of the input impedance at frequencies $\omega_k = \frac{k}{N\Delta_t}$, $k = 0, \ldots, N-1$ with the fast Fourier transform (fft) by

$$Z_{\text{in,num}}(\omega_k) = \frac{\{\text{fft}\, \mathbf{p_0}\}_k}{S_0\{\text{fft}\, \mathbf{v_0}\}_k}, \qquad (20)$$

where $\mathbf{p_0} = \{p_0^n\}_{n=0}^{N-1}$ and $\mathbf{v_0} = \{v_0^n\}_{n=0}^{N-1}$. We assume that the cross-sectional area $S(x)$ depends on a set of parameters $\Pi = \{\pi_1, \ldots, \pi_d\}$, hence $S(x) = S(x, \Pi)$. Since the function S appears in the models (1) and (4) as well as in the numerical scheme (15) - (18), also the functions P, V, p and v and the numerical approximations p_n^m and v_n^m depend on the shape parameter set Π. Moreover, all functions further depend on the length L of the tube. Of course, this also holds for the computed input impedance, hence $Z_{\text{in,num}}(\omega_k) = Z_{\text{in,num}}(\omega_k, \Pi, L)$. Given a reference impedance $Z_{\text{in,ref}}$ of a given bore, we want to estimate the parameter set Π and the length L such that $Z_{\text{in,num}}$ is close to the reference value at $\omega_k, k = 0, \ldots N^* - 1$. The numerically computed input impedance is an approximation to the input impedance only for $k < \frac{N}{2}$ and more accurate for low frequencies, hence we only take $\omega_k, k < N^*$ into account for the comparison, where $N^* < \frac{N}{2}$. To this end, we are minimizing the function

$$f(\Pi, L) = \sum_{k=0}^{N^*-1} |Z_{\text{in,ref}}(\omega_k) - Z_{\text{in,num}}(\omega_k, \Pi, L)|^2 \qquad (21)$$

with respect to the variables $\pi_1, \ldots, \pi_d$ and L. Starting from initial values Π^0 and L^0, the Levenberg-Marquardt method [13, Chapter 10] iteratively computes Π^j and L^j, $j = 1, 2, \ldots$, which are approximations to a local minimum of f. The algorithm stops as soon as the difference between two consecutive approximations is smaller than a given tolerance. Convergence to a local minimum requires a good starting point for the iteration. In this case any cylindrical tube with a plausible wind instrument radius proved sufficient for convergence to the desired minimum[1].

[1] Alternatively the Rosenbrock optimisation method [9] can be used that may identify the global minimum of a search space.

5. NUMERICAL EXPERIMENTS

In our numerical experiments, we model an alto saxophone mouthpiece adjuncted to a neck as a concatenation of a cylinder and a frustum of a cone. The mouthpiece itself is modeled as a cylinder attached to a frustum, the neck as a single frustum with the same aperture. The radial bore profile of a concatenation of a cylinder and a cone is described by

$$r(x, \Pi) = \pi_1 \qquad \text{for } 0 \le x \le \pi_4 \qquad (22a)$$

$$r(x, \Pi) = (x - \pi_4)\pi_3 + \pi_2 \qquad \text{for } \pi_4 \le x. \qquad (22b)$$

The cross-sectional area is given by $S(x) = r(x)^2\pi$. The reference input impedance is simulated with ARTool [14], using a frequency-domain plane wave model that includes viscothermal losses [4]. The corresponding parameters of the model (22), as well as the length of the tube, are given in the last column of Table 1.

We are using the profile model (22) in a first experiment, hence we want to estimate the parameters $\pi_1, \ldots, \pi_4$ as well as the length L. We start from the initial shape of a cylinder of radius 5mm and length 230mm. After 61 steps, the Levenberg-Marquardt method stops. Figure 1 shows the initial input impedance and the initial bore profile, as well as the input impedances and bore profiles of the reference and the result after the parameter optimization. The results of the Levenberg-Marquardt method are summarized in Table 1.

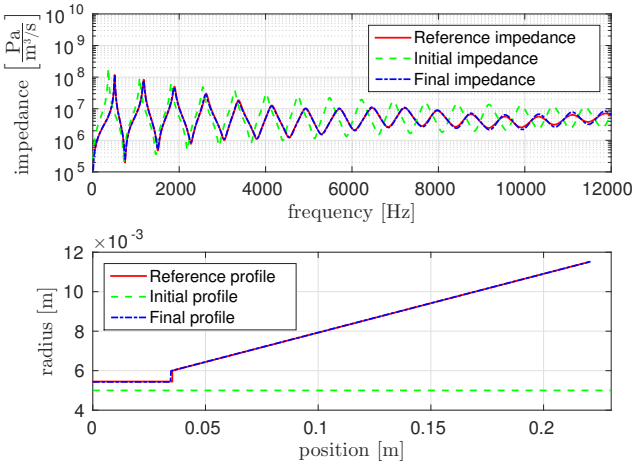

Figure 1. Reconstruction of instrument length, radii, and aperture of the cylinder-cone model (22).

Without prior information on the bore, one can model the profile by a linear interpolation through the points (x_l, π_l), $l = 1, \ldots, d$ for fixed $0 = x_1 < x_2 < \ldots < x_d$. Therefore

$$r(x, \Pi) = \frac{x - x_{l-1}}{x_l - x_{l-1}}(\pi_l - \pi_{l-1}) + \pi_{l-1} \text{ for } x_{l-1} \le x < x_l \qquad (23a)$$

$$r(x, \Pi) = \frac{x - x_{d-1}}{x_d - x_{d-1}}(\pi_d - \pi_{d-1}) + \pi_{d-1} \text{ for } x_d < x. \qquad (23b)$$

In a second experiment we take 20 uniformely distributed nodes, $x_l = \frac{l-1}{19}220 \times 10^{-3}, l = 1, \ldots, 20$. Again, as starting

	Initial (step 0)	Final (step 61)	Reference
L	230 mm	220.84 mm	220 mm
π_1	5 mm	5.4329 mm	5.45 mm
π_2	5 mm	5.9861 mm	6 mm
π_3	0	0.029739	0.029778
π_4	40 mm	34.566 mm	35.3 mm

Table 1. Summary of the reconstruction algorithm.

point we choose a cylinder of radius 5mm and length 230mm, i.e. $\pi_l^0 = 5 \times 10^{-3}$ for $l = 1, \ldots, 20$ and $L^0 = 230 \times 10^{-3}$. After 41 steps, the stopping criterion is satisfied. The initial, the reference and the final input impedances as well as the corresponding bore profiles are shown in Figure 2.

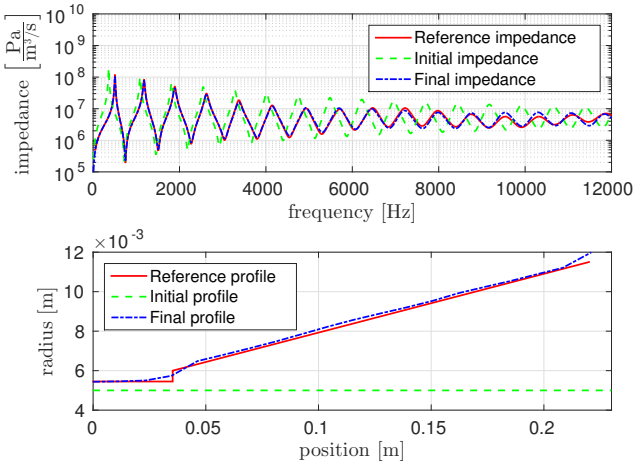

Figure 2. Reconstruction of instrument length and radii of linear interpolation model (23).

6. CONCLUSIONS

In this paper we study time-domain models for acoustic tubes, introducing a semi-analytic variant for the computation of viscothermal losses. It is demonstrated that impedances computed by time-domain models are in good agreement with reference impedances computed by plane wave frequency-domain models. Further, we describe an algorithm for the estimation of bore shape parameters using a time-domain model. Fine tuning the bore radius also updates the relevant parameters in the terms that model viscothermal and radiation losses. Current research focuses on performing the optimisation based on time-domain pressure measurements in order to estimate both the geometry of the instrument, as well as the parameters related to the player-instrument interaction.

7. ACKNOWLEDGEMENTS

This research is supported by the Austrian Science Fund (FWF): P28655-N32.

REFERENCES

[1] A. H. Benade, "On the propagation of sound waves in a cylindrical conduit," *JASA*, vol. 44, no. 2, pp. 616–623, 1968.

[2] D. H. Keefe, "Acoustical wave propagation in cylindrical ducts: Transmission line parameter approximaions for isothermal and nonisothermal boundary conditions," *JASA*, vol. 75, no. 1, pp. 58–62, 1984.

[3] L. R. Rabiner and R. W. Schafer, *Digital processing of speech signals*, ser. Prentice-Hall signal processing series. Englewood Cliffs, N.J. Prentice-Hall, 1978.

[4] J. A. Kemp, "Theoretical and experimental study of wave propagation in brass musical instruments," Ph.D. dissertation, University of Edinburgh, 2002.

[5] S. Bilbao and R. Harrison, "Passive time-domain numerical models of viscothermal wave propagation in acoustic tubes of variable cross section," *JASA*, vol. 140, no. 1, pp. 728–740, 2016.

[6] S. C. Thompson, T. B. Gabrielson, and D. M. Warren, "Analog model for thermoviscous propagation in a cylindrical tube," *JASA*, vol. 135, no. 2, pp. 585–590, 2014.

[7] S. Bilbao, R. Harrison, J. Kergomard, B. Lomard, and C. Vergez, "Passive models of viscothermal wave propagation in acoustic tubes," *JASA*, vol. 138, no. 555, 8 2015.

[8] V. Chatziioannou and A. Hofmann, "Physics-based analysis of articulatory player actions in single-reed woodwind instruments," *Acta Acust united Ac*, vol. 101, no. 2, pp. 292–299, 2015.

[9] V. Chatziioannou and M. van Walstijn, "Estimation of clarinet reed parameters by inverse modelling," *Acta Acust united Ac*, vol. 98, no. 4, pp. 629–639, 2012.

[10] R. Caussé, J. Kergomard, and X. Lurton, "Input impedance of brass musical instrumentscomparison between experiment and numerical models," *JASA*, vol. 75, no. 1, pp. 241–254, 1984.

[11] S. Bilbao, *Numerical Sound Synthesis*. Chichester: Wiley, 2009.

[12] F. Silva, P. Guillemain, J. Kergomard, B. Mallaroni, and A. Norris, "Approximation formulae for the acoustic radiation impedance of a cylindrical pipe," *J Sound Vib*, vol. 322, no. 12, pp. 255 – 263, 2009.

[13] J. Nocedal and S. J. Wright, *Numerical optimization*, ser. Springer Series in Operations Research and Financial Engineering. Berlin: Springer, 2006.

[14] A. Braden, D. Chadefaux, V. Chatziioannou, S. Siddiq, C. Geyer, S. Balasubramanian, and W. Kausel, "Acoustic research tool (ARTool)." [Online]. Available: http://artool.sourceforge.net/